

EFFECTS OF LASER RADIATION ON THE CEMENTITIOUS MATERIALS – THREE CASE STUDIES

Agnieszka J KLEMM*, Kazimierz ROŻNIAKOWSKI**

* Glasgow Caledonian University
70 Cowcaddens Road, Glasgow G4 0AB, e-mail: a.klemm@gcal.ac.uk.
** Politechnika Łódzka, Instytut Fizyki
Ul. Wólczajska 219, 90-924 Łódź, e-mail: rozniakaz@p.lodz.pl

Summary: Laser processing is unarguably associated with some alterations of cementitious materials' geometrical microstructure and chemical composition. Since high temperature is involved in the laser cleaning process, the chemical composition of surfaces may change, followed by crack development and subsequent changes of roughness. The relationship between laser treatment and substrate parameters is a two-way relationship. The great variation in absorptivity of highly developed surfaces of cementitious materials results in substantial differences in their responses to laser irradiation. Paper presents selected results of three investigations on the effect of laser radiation on characteristics of porous cementitious materials.

Keywords: Laser radiation, cementitious materials, temperature effects, surface modification

1. BACKGROUND

Laser processing of cementitious materials such as surface glazing and scabbing or removal of contaminants is becoming more and more popular nowadays. Various processes taking place during the interaction of laser with cementitious materials are associated with the temperature increase on the surface of concrete. It is important therefore to briefly analyse the performance of concrete under elevated temperatures.

OPC concrete contains 70% of $\text{CaO}\cdot\text{SiO}_2\cdot(\text{H}_2\text{O})$ gel, 20% of well-crystallised $\text{Ca}(\text{OH})_2$, ettringite ($\text{CaO}\cdot\text{Al}_2\text{O}_3\cdot\text{SiO}_2\cdot 12(\text{H}_2\text{O})$), calcium aluminate monosulphate hydrated ($4\text{CaO}\cdot\text{Al}_2\text{O}_3\cdot 13(\text{H}_2\text{O})$) and some minor phases. Dehydration will start when the concrete surface is heated for considerable time and water is lost at 200°C. Table 1 below presents the physical and chemical changes occurring during the heating up of concrete [1].

In the case of instant exposure, spalling will occur due to generation of high internal steam pressure. There are two types of spalling: explosive spalling (series of pop-outs) and sloughing off concrete surface (gradual non-violent separation of the con-

crete). An important reason for spalling is the tensile stresses caused by steam attempting to reach the surface.

Table 1. The temperature regions in which damage occurs

Temperature range	Effect
Up to 400°C	Loss of physically bond water from pores and gel
400 -540°C	Dehydration of $\text{Ca}(\text{OH})_2$
570 -573°C	Conversion of quartz from α to β phase
600 -700°C and above	Decomposition of C-S-H*
800°C and above	Decarbonation of CaCO_3
1150 - 1200°C and above	Melting

*C-S-H means amorphous calcium silicate hydrates

Thermal compressive stresses, and compression from static load parallel to the surface, increase the explosive spalling. In the case of traditional concrete (without ultra fine particles smaller than the cement grains, such as silica fume), spalling does not occur when moisture is lower than 3% by weight. Near the critical point of steam (374°C), spalling often occurs. Above this point, pores cannot have liquid and vapour together, and pressures increase considerably. Thermal stresses sufficient for spalling can be unloaded by thermal cracks [2].

Rapid temperature increase during laser exposure may lead also to noticeable modification of surface chemical composition. Changes in the composition of cementitious surfaces may be associated with the following processes:

- Dehydration starting as soon as surface gets heated, and water loss at 200°C. The dehydration of $\text{Ca}(\text{OH})_2$ follows shortly after 420°C is reached and is represented by the following equation: $\text{Ca}(\text{OH})_2 \rightarrow \text{CaO} + \text{H}_2\text{O}$

- Breakdown of hydrated chemical bonds starting at around 550°C with a complete break down at 800-900°C. Decarboxylation of Ca₂CO₃ occurring at around 700°C.
- Creation of stable ceramic bond (glazing) such as CaO·SiO₂·2CaO·SiO₂, anorthite (CaO·Al₂O₃·2SiO₂), and rankinite (3CaO·2SiO₂) starting at around 1600°C (Lin SPIE 1994) [3].

Schmidt and Li [4] carried out X-ray diffraction (XRD) experiments on B45 concrete exposed to Nd:YAG laser irradiation. The ratio between XRD peaks of SiO₂ and CaCO₃ appeared to increase from 27:100 to 200:100, when a Nd:YAG laser was applied at 1064 nm with a fluence of approximately 14 J/cm². A vast amount of CaCO₃ has therefore disappeared from the processed area. At the same time, the peak ratio obtained for wavelength of 532 nm was equal to 55:100, being more similar to the original surface. The structural and chemical makeup of the laser processed surface was changed significantly when 1064nm wavelength rather than 532nm was applied.

The removal depth per pulse can be obtained by the following equation based on the Beer Lambert analysis:

$$H_p = \frac{1}{\alpha} \ln \frac{F}{F_T} \quad (1)$$

Where, H_p (cm) is the removal depth per pulse, F (J/cm²) is the incident fluence; F_T (J/cm²) is the threshold fluence and α is the extinction/absorption coefficient (1/cm). The thermal loading γ (kJ/cm³) of the material can be represented therefore as follows [1]:

$$\gamma = F_T \alpha \quad (2)$$

Where $1/\alpha$ is an absorption length.

The threshold value of the fluence, at which significant material removal occurs can be defined as:

$$F_T = \frac{H + \rho C_p T_d}{\alpha(1-R)} \quad (3)$$

Where, H is the latent heat of fusion (J/kg), ρ is the density (kg/m³), C_p is the specific heat (J/mol K) and R is the reflectivity (%) and T_d is a critical temperature (K) at which rapid thermal degradation of the material takes place, leading to the production of volatile fragments.

The experimental investigations by Schmidt and Li [4] revealed that the increase of strength of concrete results in decrease of absorption length, threshold fluence and thermal loading (Table 2).

Table 2. Comparison of the ablation values.

Material	F_T (J/cm ²)	α (cm ⁻¹)	γ (kJcm ⁻³)	α^{-1} (μ m)
B45	0.45	2.52*10 ⁴	11	0.396
B55	0.17	3.01*10 ⁴	5	0.331

According to the research by Rao et al. [5], a high power laser beam incidencing on a concrete surface can lead to spalling, glazing, or vaporization, depending upon the laser power density

and scan speed. Table 4 shows the effect of the CO₂ laser on the concrete. As the power density and laser scanning speed changes, the effect of laser on the concrete changes - spalling, glazing, cutting, and drilling of concrete.

Table 3. Effect of CO₂ laser on the concrete.

Effect of laser	Power density (W/ cm ²)	Scanning speed (mm/min)
Spalling	40-200	150-1000
Glazing	300 or above	25-450
Cutting by re-peated glazing	2000	600
Drilling	1200-3000	Angle of incidence 30°

Matsui and others [6] carried out research on laser cleaning of concrete by using the CO₂ laser. They observed some pop-outs and cracks caused by the sudden temperature increases on the concrete surface. The porosity and the moisture contents work together and affect the laser cleaning process. When a high power density laser was applied to wet, low porosity mortar, pop-out occurred. In the case of absolutely dry mortar, with low water cement ratio, hair cracks occurred in the high-energy irradiation zone. No damage occurred in mortar specimens with high porosity (high water cement ratio) and low energy.

According to research by Lawrence [7], pore formation is one of the features in the laser-glazed surface. Fig. 1 shows the pores formed and cracking when a CO₂ laser (power densities: 2.25 kW/cm², traverse speeds: 240 mm/min and laser spot diameters: 10 mm) was applied to a concrete surface. The mechanism behind the pore formation is mainly attributed to gas escaping from the melting concrete. At a given laser power density, porosity decreases with the increase of the scan speed. Different lasers affect the concrete in different ways despite the similar power densities.



Fig. 1. Typical optical surface morphology of the OPC surface glaze generated with the CO₂ laser (Lawrence, 2004).

Fig. 2 shows an OPC surface glaze generated by a high power diode laser (HPDL). The glaze is of a fully amorphous nature (no discernible structure) while the glaze generated by the CO₂ laser is of a semi-amorphous nature (randomly located regular columnar structure). In contrast, the untreated OPC comprises of a porous polycrystalline structure.

Lawrence and Li [8] investigated the effect of laser application to the concrete surface on the sorptivity of the concrete. The sorptivity of concrete becomes low, when concrete is treated

with high power laser. It is mainly because of the glazing of concrete. Figure 3.14 shows the water sorptivity of the untreated OPC surface and the laser (power: 120W, power densities: 1 kW/cm^2) treated surface.

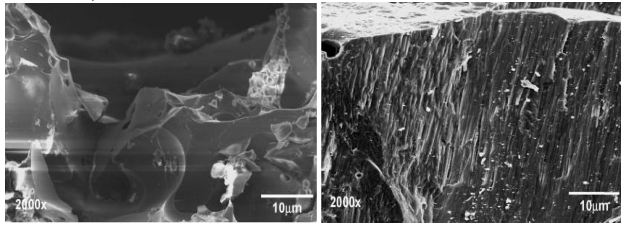


Fig. 2. Typical SEM micrograph of the fracture section of the OPC surface glaze generated by the HPDL (left) and the CO_2 laser (right) (Lawrence, 2004).

The sorptivity of the untreated surface was $0.096\text{ mm/min}^{1/2}$, compared with $0.043\text{ mm/min}^{1/2}$ for the laser treated surface. Thus, the laser treated OPC surface has half the sorption of the untreated one and, therefore, twice as much resistance to water absorption.

2. EXPERIMENT

2.1. Study 1

Significant alterations of surface properties are unarguably associated with high energy laser radiation. The application of the impulse energy of 35 J with duration 3ms generated by the Nd:YAG laser (wavelength $\lambda = 1.06\ \mu\text{m}$) lead to the formation of characteristic laser spots, seen on the photograph (Fig. 3). Micro-craters consist of centrally placed areas from which material has been removed and the surrounding area (ring) of relatively small damage. The subjects of presented investigation were concrete samples with compressive strength - 30MPa and 85MPa [9].



Fig. 3 Photograph of a sample with craters.

The SEM photographs (Fig. 4) of the surfaces before and after laser treatment show clear differences in surface microstructure. Some compounds from the affected areas have been removed due to evaporation or high gas pressure. It is possible to distinguish fragments of material with an oval, unordered shape which could be created as a result of melting and recrystallising.

Table 4 shows the chemical analysis of non-exposed areas, areas from the bottom of craters and on their slopes. Significant fluctuations of chemical composition within the laser-affected area were observed.

The percentage of silica in the original concrete surface was comparatively low, with the higher value at the bottom of the crater and its maximum on the slope. The same fluctuations were also observed for other compounds (Al, Fe).

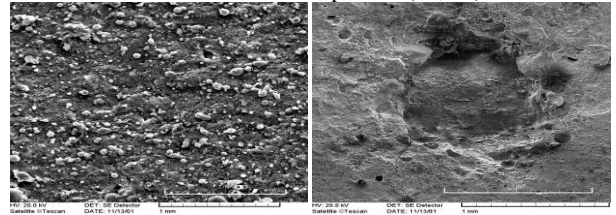


Fig. 4. SEM image of non-exposed (left) and exposed sample (right)

Table 4. Concentration of different element on concrete surfaces.

Element	30 MPa concrete			85 MPa concrete		
	Non-exposed area	Bottom of crater	Slope of crater	Non-exposed area	Bottom of crater	Slope of crater
C	18.88	15.33	10.77	11.52	10.01	9.31
O	14.21	50.19	53.34	50.41	51.8	55.39
Mg	0.44	0.54	0.53	0.54	0.48	0.52
Al	0.89	0.88	1.78	1.66	1.39	3.1
Si	4.67	4.33	14.38	5.93	7.14	11.1
S	0.31	0.25	0.49	0.30	0.63	0.98
K	0.36	0.47	0.46	2.67	1.28	0.9
Ca	24.68	27.53	17.11	25.47	26.22	16.66
Fe	0.57	0.49	1.08	1.08	0.62	1.16

The results of linear analysis give the evidence that the greatest fluctuations of chemical analysis take place on the slope of the crater. It is particularly pronounced for Aluminium (Al), Silica (Si) and Calcium (Ca). Fluctuations of chemical composition at the bottom of crater and on the surrounding crater surface are negligible. Optical microscope investigations did not reveal any significant differences between samples of different compressive strengths

Investigation confirmed that in the close neighbourhood of craters only a slight damage of external layer of material took place with no evidence of material cracking. It may suggest that this process can only be relevant in the initial phase of heating and only in the central part of crater. Spalling of material from crater seems to be intensified by this process. A small crack of the material can be seen in the left bottom part of the crater on Fig.2 above.

2.2. Study 2

In the second investigation concrete samples of 30MPa and 50 MPa were exposed to CO_2 laser radiation (wave length $\lambda = 10.6\ \mu\text{m}$). Samples were subjected to laser exposure of increasing power from 0.2 kW – 1.6 kW [10].

Figure 5 shows the photograph of the sample (C30) with clearly visible laser grooves consisting of centrally placed area from which material has been removed and the surrounding area of relatively small damage. Maximum depth of penetration was between 1.0 – 4.8 mm depending on the laser power.

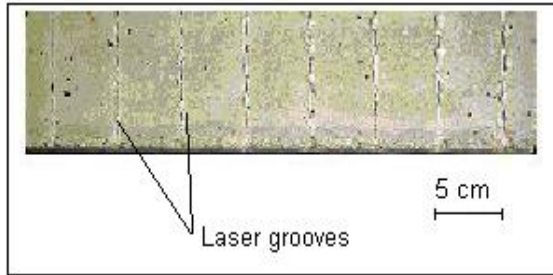


Fig. 5. Sample after exposure to laser irradiation (C30)

The depth of penetration recorded for the increasing laser energy from 0.2 to 1.0 kW for both samples is of the similar order (Table 5). Further increase above 1 kW results in more severe effect on lower strength sample (C30).

Table 5. Depth of laser beam penetration

Power [kW]	0.2	0.4	0.6	0.8	1.0	1.2	1.4	1.6
Depth [mm]								
	C 30	1.0	1.8	2.4	3.0	3.0	3.4	4.0
	C 50	1.1	1.8	2.6	3.0	3.1	3.0	3.5

Similarly to the previously presented investigation fragments of amorphous material of irregular shape were created as a result of melting and re-crystallising. Figures 6-7 show the effect of high power laser on cementitious surfaces.

Experiment proved that the relatively low power of laser radiation (below 1.0 kW) does not have any significant effect on concrete performance regardless its composition and variation in microstructure. However further increase in energy results in more pronounced changes in concrete of lower strength. High power exposure has resulted in some decolourisation of material near laser groove as well as creation of micro-cracks due to temperature gradients.

Chemical analyses of concrete surfaces were performed in three points within: non-exposed area, fracture area below laser groove and the area of new created material Table 6.



Fig. 6. Concrete sample C30 exposed to 1.6 kW



Fig. 7. Concrete sample C50 exposed to 1.6 kW

Table 6. Chemical composition

Element	Concrete 30			Concrete 50		
	Non-exposed	Cross section	New Material	Non-exposed	Cross section	New Material
C	8.89	9.38	7.44	12.60	8.36	6.99
O	50.46	48.62	47.44	48.55	50.79	49.54
Mg	0.46	0.39	0.29	0.41	0.34	0.48
Al	1.19	1.17	0.86	1.03	0.99	1.23
Si	10.49	10.78	29.71	17.35	21.87	24.64
S	1.32	1.12	-	1.09	0.83	0.30
K	1.34	0.81	0.25	1.44	0.91	0.53
Ca	24.97	26.94	13.34	17.04	15.35	15.81
Fe	0.88	0.79	0.66	0.48	0.56	0.47

Significant fluctuations of chemical composition of non-exposed surfaces and “new” surfaces have been recorded in both cases. This is especially visible for silica and calcium. While percentage of silica increases as a result of laser radiation, amount of calcium decreases. Relatively small variations between non-exposed areas and cross sectional analysis below direct laser impact were observed with more pronounced changes for samples of higher porosity and lower strength.

2.3. Study 3

The third investigation deals with application of Nd:YAG laser (fluence 3.06 J/cm²). for cleaning of cementitious surfaces. Graffiti covered mortar samples with different internal microstructures (HP - high porosity; LP - low porosity), surface roughness: A (Ra = 2.28 - 2.49µm), B (Ra = 7.70 - 8.49µm) and C (Ra = 15.58 - 17.89µm), and moisture content (DRY, WET) were cleaned and analysed [11,12]. A separate set of samples of highest roughness (set C) was subjected to 600 alternated freezing/thawing cycles (-20°C to +20°C). Exposure resulted in increased surface roughness Ra = 15.79-18.13µm. Surface roughness was measured by a stylus device and represented by the average surface roughness (Ra).

The increase of mortar temperature and subsequent thermal stresses and internal pressure development leads to the formation of cracks. Different types of cracks such as closed cracks

(spalling), cracks from pit-hole and open cracks were observed on the laser-cleaned areas, depending on the surface conditions (Fig. 8). Open cracks were mainly caused by thermal stresses on mortar surfaces, while closed cracks were caused by internal pressures of water/air inside the pores. Furthermore, when the pit-hole is exposed to laser treatment, the temperature increase at the mortar surface is higher than at the bottom of pit-hole because of its profile. Cracks may therefore easily propagate from the pit-hole as shown in Figure 8 (b).

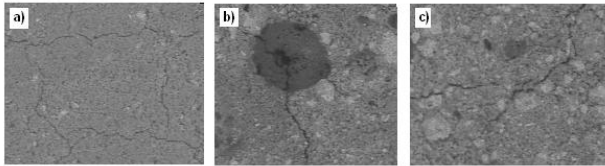


Fig. 8. Different types of cracks (1000x): a) Closed crack (spalling) - LP-A(WET); b) Crack from pit-hole - HP-C(DRY); c) Open crack - HP-C(DRY).

Heat produced by laser cleaning on mortar surfaces dissipates through formations of cracks, glazing, removal of paint or mortar and other losses. The amount of energy dissipated through the crack development or mortar removal depends on the properties of mortar. In weaker surfaces, it was shown that there is a great potential to dissipate the energy through the removal of mortar rather than through the development of cracks. The mortar surface exposed to freezing and thawing cycles was found to be weaker than that of the laboratory-cured sample, and consequently no cracks were observed here (Fig.9).

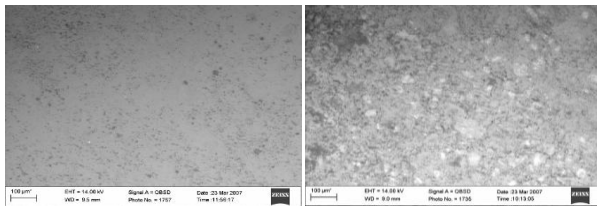


Fig. 9. BSE images (150x) of mortars subjected to F/T cycles before and after the application of 31 laser pulses.

Near-surface porosity of laser-cleaned areas was assessed qualitatively by the analyses of BSE images. Two different zones within laser craters were identified and analysed: Undamaged Zone and Damaged Zone. The damaged zone was found to be denser and more consolidated than either the undamaged zone or the reference surface, due to vitrification of some parts of mortar surface following the laser cleaning process. Furthermore, near surface porosity of reference surface seemed to be higher than the undamaged laser cleaned area (Fig. 10 (a) and (b)).

In the damaged zone, glassy patches were observed where cracks and pores formed during vitrification. Pore formation results here mainly from gas escaping from melted cement paste. Despite the formation of pores, the near-surface porosity of glassy patches seems to be lower than in the remaining mortar surface.

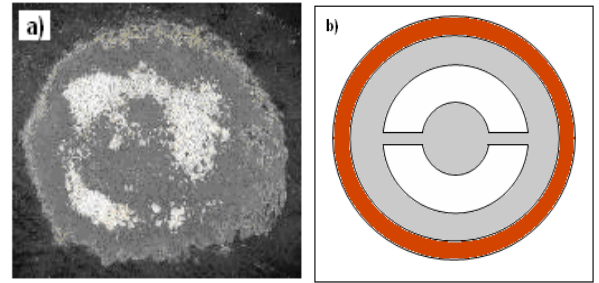


Fig. 10. Laser crater: (a) Optical micrographs of LP-A(DRY) after 6 pulses (80x); (b) Different zones within the laser crater.

The main elements of cementitious composites are Ca, Si, Al, Fe, and S. The changes in concentration of Al, Fe, and S on mortar surfaces seem to be insignificant, and subsequently only Ca and Si have been considered in this analysis.

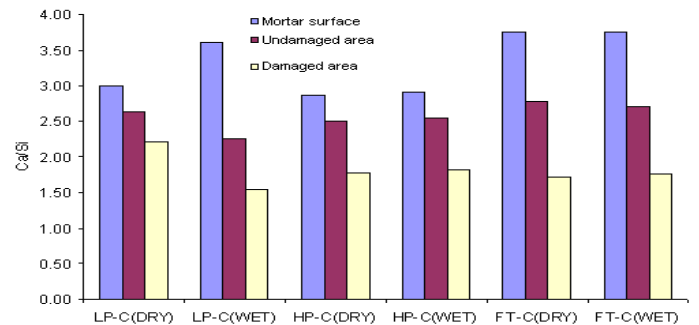


Fig.11. The value of Ca/Si ratio on surfaces of mortar samples

Chemical analyses of surfaces focused on two different zones. The EDX analysis of laser-affected areas showed that the ratio of Ca/Si obtained from damaged zone was higher than for the undamaged zone or the reference surface. Moreover, the value of Ca/Si in the undamaged zone was higher than for the reference surface (Fig. 11). The average value of Ca/Si on the laser-cleaned area was found to be 47% lower than on the reference mortar surface. Hence laser-cleaned mortar surface was found to be high in Si element and/or low in Ca element when compared with the original mortar surface.

Increment of Si content with respect to Ca on mortar surfaces could be attributed to the removal of CaCO_3 or movement of SiO_2 to mortar surfaces. Another possible reason could be associated with changes in the relative distribution of melted cement paste and aggregate and therefore relative elemental abundance in the near-surface layer.

Even though there was no sign of paint on the optical micrograph in laser-cleaned areas, the concentration of carbon was higher than on the reference surface. The average amount of carbon in the laser-cleaned areas was found to be around 56 % higher than on reference surfaces, despite the fact that mortar removal was visible. It is therefore clear that the removal of paint from rougher surfaces cannot be fully-achieved without damaging the mortar surface.

Curing condition and near-surface porosity seem to have some influence on the amount of residual paint on laser-cleaned surfaces. Since samples exposed to 600 freeze/thaw cycles have, a higher number pores and cracks in the near-surface layer, penetration of paint is high, and the amount of carbon was found to be around 42% higher than on the surfaces of laboratory-cured samples. Furthermore, the amount of carbon after laser cleaning the laboratory-cured, highly porous samples was around 14% higher than for the laboratory-cured, low porous mortars. This indicates that laser cleaning of highly porous samples is more problematic.

3. FINAL REMARKS

During the last couple of decades laser processing of cementitious materials, such as surface glazing, scabbing or removal of contaminants has been gradually becoming more and more popular. The laser treatment is unarguably associated with some moderations of material's geometrical microstructure and chemical composition. Since high temperatures are involved the chemical composition of surfaces may change, followed by crack development and subsequent alteration of roughness. Despite the fact that these effects are generally microscopic and only visible at high magnification, their importance should not be underestimated as they may expose surfaces to further accelerated environmental deterioration

The results presented here highlight the potential application of laser beam radiation for the removal of surface layer of material and substantial modification of surface. New material created in the area of laser interaction as a result of melting and recrystallizing can play an important part in protection process against the effect of weathering factors. Glassy surfaces with different characteristics than the base material, with lower permeability and poor adhesion should effectively protect concrete against the aggressive environment as well as acts of vandalism (unwanted graffiti). Nevertheless, without a comprehensive database governing principal mechanical and microstructural characteristics, and the effect of laser radiation, it will not be possible to further advance the treatment and make it available on industrial scale.

References

- [1] Schmidt, M. J.J., Li L., Spencer J.T. *An investigation into the feasibility and characteristics of using a 2.5k W high power diode laser for paint stripping*. Journal of Materials Processing Technology 138 (2003) 109-115.
- [2] Georgali, B., Tsakiridis P.E. *Microstructure of fire damaged concrete. A case study*, Cement and Concrete Composites 27(2) (2005) 255-259.
- [3] Lin L.L., Steen W.M., Modern P.J. and Spencer J.T., *Laser removal of surface embedded contaminations on/in building structures*, Laser Materials Processing and Machining, SPIE: 2246, 1994.
- [4] Schmidt M.J.J., Li L. *Surface modification of OPC- based cent using a frequency doubled Nd:YAG laser system*. Applied Surface Science 186 (2002).

- [5] Rao, B. T., H. Kumar and A. K. Nath., *Processing of concretes with a high power CO₂ laser*. Optics & Laser Technology 37 (2005) 348–356.
- [6] Matsui, I., Nagai K., Yuasa N., Ishigami Y. *Removing graffiti on concrete surface by laser*. Proceeding of the International Congress “Challenges in Concrete Construction” Dundee, 2002.
- [7] Lawrence, J., *A comparative analysis of the wear characteristics of glazes generated on the ordinary Portland cement surface of concrete by means of CO₂ and high power diode laser radiation*, Wear 257 (2004) 590–598.
- [8] Lawrence, J. and Li L. *The effects of process gas type on the surface condition of high-power diode laser-treated ordinary Portland cement*. Optics and Lasers in Engineering 36 (2001) 599–605.
- [9] Klemm P, Roźniakowski K, Klemm A J *Some experimental results of interaction of strong impulse of laser radiation with the surfaces of high performance concrete* Proceedings of the 7th International Conference on Structures under Shock and Impact”, Montreal 2002
- [10] Klemm A J, Klemm P, Roźniakowski K *Modification of concrete surfaces by laser radiation* ICCRRR 2005, Cape Town, South Africa
- [11] Sanjeevan P, Klemm A J, Klemm P *Removal of graffiti from the mortar by using Q-Switched Nd:YAG Laser* Applied Surface Science, 253(20) (2007) 8543-8553
- [12] Klemm A. J., Sanjeevan P., Klemm P. *Micro-scale alterations of cementitious surfaces subjected to laser cleaning process and their potential impact on long term durability* 2nd ICCRRR 2008, Cape Town, South Africa